THE JOURNAL OF THE TEXTILE INSTITUTE, 2018
https://doi.org/10.1080/00405000.2018.1437113

Taylor & Francis
Taylor & Francis Group

Evaluating the fabric performance and antibacterial properties of 3-D piezoelectric spacer fabric

Derman Vatansever Bayramol[a], Navneet Soin[b], Amrita Dubey[c], Ravi Kant Upadhyay[d], Richa Priyadarshini[c], Susanta Sinha Roy[d], Tahir H. Shah[b] and Subhash C. Anand[b]

[a]Department of Textile Engineering, Namik Kemal University, Corlu-Tekirdag, Turkey; [b]Institute for Materials Research and Innovation, University of Bolton, Bolton, United Kingdom; [c]Department of Life Sciences, School of Natural Sciences, Shiv Nadar University, Noida, India; [d]Department of Physics, School of Natural Sciences, Shiv Nadar University, Noida, India

ABSTRACT

The increasing need of on-demand power for enabling portable low-power devices and sensors has necessitated work in novel energy harvesting materials and devices. In a recent work, we demonstrated the production and suitability of three-dimensional (3-D) spacer all fibre piezoelectric textiles for converting mechanical energy into electrical energy for wearable and technical applications. The current work investigates the textile performance properties of these 3-D piezoelectric fabrics including porosity, air permeability, water vapour transmission and bursting strength. Furthermore, as these textiles are intended for wearable applications, we have assessed their wear abrasion and consequently provide surface resistance measurements which can affect the lifetime and efficiency of charge collection in the piezoelectric textile structures. The results show that the novel smart fabric with a measured porosity of 68% had good air (1855 l/m^2/s) and water vapour permeability (1.34 g/m^2/day) values, good wear abrasion resistance over 60,000 rotations applied by a load of 12 kPa and bursting strength higher than 2400 kPa. Moreover, the antibacterial activity of 3-D piezoelectric fabrics revealed that owing to the use of Ag/PA66 yarns, the textiles exhibit excellent antibacterial activity against not only Gram-negative bacteria *E. coli* but they are also capable of killing antibiotic methicillin-resistant bacteria *S. aureus*.

ARTICLE HISTORY
Received 9 August 2017
Accepted 1 February 2018

KEYWORDS
Piezoelectric; spacer fabric; properties

Introduction

Spacer fabrics are considered to be the next generation of technical textile structures which can be produced by weaving (Großmann et al., 2010; Li, Wang, Zhang, & Wu, 2009; Mountasir, Hoffmann, & Cherif, 2011; Ünal, 2012), warp knitting (Liu, Hu, Long, & Zhao, 2012; Ye, Fangueiro, Hu, & de Araújo, 2007; Ye, Ho, & Feng, 2008), weft knitting (Delkumburewatte & Dias, 2009; Dias, Monaragala, Needham, & Lay, 2007; Liu & Hu, 2011; Shepherd, 2004) and non-woven (Fangueiro & Soutinho, 2013; Gong, Dong, & Porat, 2003) technologies. A spacer fabric consists of two outer layers and a spacer layer of filaments (mono- or multi-) connecting the two outer layers to either join them together or to keep them apart. For knitted spacer fabrics, the outer layers consist of weft/warp-knitted yarns which can be of the same or different materials. Due to the three-dimensional (3-D) structure, knitted spacer fabrics have found use in a number of applications including but not limited to vibration isolation (Chen, Liu, & Hu, 2016), compression bandages (Anand & Rajendran, 2011; Pereira, Anand, Rajendran, & Wood, 2007), prevention of chronic wounds (Wollina, Heide, Müller-Litz, Obenauf, & Ash, 2003; Wollina, Heide, & Swere, 2002) and more recently in energy harvesting (Soin et al., 2014). Using 3-D knitted fabric as an energy generator for the conversion of mechanical energy of environment and human activities is one of the most recent area of research for 3-D fabric technologies. The first 3-D piezoelectric fabric, utilising the piezoelectric effect for the conversion of mechanical to electrical energy consisted of high β-phase (~80%) piezoelectric poly(vinylidene fluoride), PVDF monofilaments (300 dtex) as the spacer yarn interconnected between silver (Ag) coated polyamide multifilament yarn (143/34 dtex) and polyester (84 dtex) layers acting as the top and bottom electrodes (Soin et al., 2014). The output power density of these 3-D textiles were reported to be in the range of 1.10–5.10 μWcm^{-2}, when subjected to an impact of 0.02–0.10 MPa, and is significantly higher than the existing 2-D woven and non-woven piezoelectric structures (Fang, Niu, Wang, Wang, & Lin, 2013; Soin et al., 2014; Zeng et al., 2013). Such materials are generally named as '*smart materials*', with the ongoing research mostly focusing on enhancing their efficiency. However, for wearable energy harvesters, the thermo-physiological properties of such structures are of equal importance and can potentially dictate their most appropriate application and further uptake as apparel or technical fabrics (Bayramol et al., 2017; Soin, Anand, & Shah, 2016).

One of the biggest advantages of 3-D spacer textiles is that the main layers can be manufactured from various yarns having

CONTACT Derman Vatansever Bayramol dvbayramol@nku.edu.tr; Navneet Soin n.soin@bolton.ac.uk

different properties (conductive, antibacterial, heat resistant, etc.), while the spacer monofilament can have entirely different property altogether. In the case of wearable spacer textiles, thermo-physiological comfort properties are highly desirable to facilitate the transport of the heat and moisture away from the skin and maintain the breathability of the fabric through sufficient air ventilation (Yang & Hu, 2016). In the case of smart 3-D piezoelectric textiles intended for wearable and insole applications while creating and transferring the piezoelectric charge accounts for the power generation, a comfortable fabric which normalises the heat transfer during the mechanical impact by human body is simultaneously desired. For a multi-component textile structure as this, the repeated mechanical compression and impact required for charge generation will affect the fabric wear and lifetime. Apparel or technical fabric, it is very likely that they will undergo some mechanical impacts which will affect the fabric wear and lifetime. Therefore, wear resistance of the fabrics should be investigated together with comfort properties (Crina, Blaga, Luminita, & Mishra, 2013; Rajan, Souza, Ramakrishnan, & Zakriya, 2016). For textile structures, either apparel or technical, their fabric performance is as much important as their underlying smart behaviour, such as piezoelectric behaviour in this case.

As compared to the traditional methods of textile production such as weaving, knitting, non-wovens; the 3-D spacer fabric production is a relatively new fabric production technique and as such there is only a limited amount of reported work on their fabric properties. Especially, the thermo-physiological properties of smart technical textiles have not been reported before in the literature. In this work, we have measured the fabric performance parameters such as air permeability, wear abrasion, water vapour transmission and antibacterial of the 3-D energy harvesting piezoelectric fabrics. Additionally, we have also performed the surface resistance measurement of the fabrics at various stages of wear abrasion and observed the fraying nature of Ag/PA66 fibres which can potentially affect the performance of the charge gathering capability. For smart textiles which can enable future wearable technologies, it is important to assess these fundamental properties in order to assess their suitability for long-term use. Most of the recent research is now focused on the development of multifunctional smart materials which can exhibit multiple properties and functionalities. The 3-D spacer piezoelectric textile structure is a good example of such multifunctional smart textiles wherein it can be used complementarily in most places where an ordinary textile structures can be used and in terms of functionality it can generate an electrical charge upon an applied mechanical stimulus, while also preventing the user from bacterial infections.

Experimental procedure

Materials

The 3-D piezoelectric fabrics were produced on an E20 circular weft knitting double-jersey machine at Baltex Speciality Knitters Ltd. Derbyshire, United Kingdom. A commercially available Ag coated PA66 conductive yarn (Shieldex, 143/34 dtex) was used in the knitted body together with an insulating polyester (84 dtex) yarn. Piezoelectric PVDF monofilaments (300 dtex) were used as a spacer yarn between two knitted faces of the 3-D fabric structure. Further technical details of the PVDF yarn including the synthesis procedure alongside their crystalline, microstructural, piezoelectric properties can be found in our earlier work (Soin et al., 2014).

Methods

All fabric performance tests were carried out in laboratory conditions where the relative humidity and temperature are kept 65% ± 2 and 20 °C ± 2 °C, respectively. Samples were kept in laboratory conditions for at least 24 h before the tests. Fabric thickness of the 3-D piezoelectric knitted fabric was measured by a Karl Schröder KG thickness gauge which uses EN ISO 5084 standard. Mass per unit area (g/m^2) of the fabric sample was measured using precision scales. The bursting strength and bursting distension of the 3-D piezoelectric fabric were determined using the hydraulic method which is based on the TS 393 EN ISO 13,938–1 test standard. The reported results are an average of triplicate measurements. For the investigation of the porosity of the piezoelectric spacer fabric, 20 × 20 mm samples were prepared and weighted, with the measurements being done in triplicate. Toluene (C_7H_8) with 99.5% purity and the density of 0.87–0.88 g/cm^3 was used to immerse the sample in wherein the idea is to use the toluene as a filler for the pores of the fabric. The samples were further weighed after the immersion process and the porosity of the complete fabric structure was calculated from the following equation (Crina et al., 2013):

$$P = \frac{\gamma_r - \gamma_a}{\gamma_r} \times 100 \quad (1)$$

where 'P' is the porosity (%), 'γ' is the areal density (g/m^2), while the subscriptions 'r' and 'a' stand for relative and apparent, respectively. The air permeability characteristics of the 3-D piezoelectric fabric were measured on PROWHITE® Airtest II equipment according to the EN ISO 9237 standard using a 20 cm^2 test head. For technical fabrics, the stipulated pressure is 200 Pa and accordingly 10 measurements were taken with the average value being reported. The water vapour transmission of the 3-D piezoelectric fabrics was investigated using PROWHITE® water vapour permeability tester. The samples with a diameter of 96 mm were prepared as indicated in BS 7209 and the mass of the samples was recorded before the test. The as-prepared samples were covered and fixed on the receptacles (83 mm inner diameter) containing 46 ml of distilled water. Each sample set-up was weighed and located on the rotating platform which rotated for 1 h with a speed of 2 rpm before the beginning of the actual test. This period is the time for transient behaviour of the fabric prior to reaching equilibrium. Each set-up was weighed and put back onto the platform for next 24 h to rotate with the same rotational speed. The test was carried out for 96 h by weighing the samples after 24th, 48th, 72th and 96th hours. After 96 h, the samples were taken off from the sample holder and weighed. The measurements were carried out in triplicate to ensure repeatability of the results. The water vapour transmission rate (WVTR) itself was calculated from the following equation (Arabuli, Vlasenko, Havelka, & Kus, 2010):

$$WVTR = \frac{G}{t.A} \quad (2)$$

where; '*G*' is the weight change in grams, '*t*' is the elapsed time in hours and '*A*' is the test area (inner diameter of the water receptacle, in m^2).

Textile materials undergo a number of friction/rubs during their everyday use during which they can get worn out resulting in damage and a consequential loss in the performance. It should be mentioned that majority of the wear abrasion occurs as a result of the fabric–fabric friction. The wear abrasion test of the 3-D fabric was carried out using a Martindale M235 abrasion and pilling tester. 3-D fabric samples were prepared as directed in ASTM D4966. The samples were rubbed against an abradant fabric with an applied weight of 12 kPa and at a speed of 47.5 rpm. The samples with a diameter of 38 mm were weighed via precision scales before and after the rubbing cycles. The samples were rubbed 60,000 times in total. After each thousand rubs, the samples were taken out, weighed and inserted back.

The surface resistance of the 3-D fabric samples was also estimated using the four-probe method, adapted to textiles, using cylindrical tips instead of point-contact tips (Stempien, Rybicki, & Rybicki, 2015). During the measurement, a constant DC current, *I*, is passed through the two outer electrodes while measuring the potential drop, *U*, occurring between the two-middle electrodes. The surface resistance, R_s is itself given by the following equation:

$$R_s = \frac{\pi.U}{ln2.I} \tag{3}$$

where R_s is surface resistance (V/sq.), *I* is current (A) and *U* is voltage (V).

The electrical characteristics of the produced 3-D fabrics have been measured by a four-point probe system from 'Everbeing Intl Corp' using a four-point probe head with a probe spacing of 1.5 mm. The diameter of the Tungsten Carbide electrode contact tip was 0.4 mm. The station was combined with a 'Keithley 2450' source meter for measuring the sheet resistance of the produced samples. The resistance measurements were carried out for samples before, during and after the abrasion tests.

For assessing the antibacterial properties of these textiles, two strains of bacteria, namely Gram-negative *Escherichia coli (E.coli)* MG1665 and Gram-positive *Staphylococcus aureus (S.aureus)* UAMS-1 have been used in the study. The *E.coli* cells were grown in Luria bertani (LB) broth (Hi-Media, Mumbai, India) at 37 °C for 24 h. *S. aureus* were cultivated in tryptic soy broth (TSB) and (TSA) agar (Hi-Media, Mumbai, India). Cells were harvested, centrifuged at 6000 rpm for 5 min and washed with sterile phosphate buffer saline (PBS) solution. Bacterial cell suspensions were then re-suspended in PBS and diluted to obtain cell samples containing ~107–108 CFU/ml which were used for further experiments. To determine the antibacterial activity against *E.coli* and *S.aureus*, 1 × 1 cm samples of the 3-D piezoelectric fabrics were used. Briefly, single swatches of fabric were dipped in bacterial cell suspensions and kept at 200 rpm to ensure proper contact. Parallel experiments were also conducted with bacterial cell suspensions without any 3-D piezoelectric fabrics to use as positive control. After 3 h, 100 µl of the cell suspension was 10-fold serially diluted and spotted on agar plates. Simultaneously, 100 µl of 10^5 dilution was taken and spread on agar plates.

Results and discussions

The cross-section scanning electron microscope image of the 3-D piezoelectric fabric sample is shown in Figure 1(b) which clearly shows the position of various fibres in the structure. Now, as compared to the conventional 2-D fabric structures, the 3-D fabrics can be considered as a relatively bulky structure, which was confirmed by the measured thickness of ~3.51 mm with a mass per unit area of 485 g/m^2. As such, these materials may be more amenable for technical applications as compared to apparel. However, the fabric may still need to be in contact or closely located to the human body in applications such as shoe insole. Again, for such applications, the comfort properties of 3-D fabrics are as important as the functionally. The porosity of the spacer fabric itself is dictated by factors such as loop length, stitch density, thickness and structure of the fabric and consequently controls the permeability and thermo-physiological properties (Rajan et al., 2016). For the 3-D piezoelectric spacer textile, the porosity, as evaluated using Equation 1 was determined to be 68 ± 1%. For an all-polyester warp-knitted 3-D spacer fabric of 3.1 mm thickness and an areal density of 491 g/m^2, a porosity value of nearly 88% was reported by Rajan et al. (2016). The air permeability of a fabric depends on structural factors such as surface finish of fabric, stitch density, thickness and type of spacer yarns while macroscopically, the number and size of pores affect the airflow through the structure. Now, if a fabric displays high porosity, it can be safely assumed that it is highly permeable. In our case, as the 3-D piezoelectric fabric structure is composed of two knitted layers of multifilament yarns with a spacer in between them, high air permeability values are expected. Consequently, the air permeability measurements for the 3-D piezoelectric fabric samples (carried out 10 times) revealed an average value of 1855 l/m^2/s. Comparatively, in their recent work, Arumugam, Mishra, Militky, Davies, and Slater (2017) have reported a value of nearly 950 l/s/m^2 for 3-D all-polyester spacer fabric. As compared to the conventional 2-D fabrics, the 3-D fabrics are more breathable and hence show higher air permeability. The high porosity of the structure contributing to the high permeability value is clearly visible in the SEM images provided in Figure 1. The high permeability has a subsequent significant impact on the ensuing comfort properties by allowing for the heat and water transfer to occur through the fabric thereby keeping the body cool.

The water vapour transfer characteristic of a textile material is an important parameter since it is directly related to the capability of the perspiration transfer. Therefore, textiles such as sport wears or shoe insoles are expected to have good water vapour transfer characteristic. The 3-D piezoelectric fabric test samples were prepared as indicated in BS7209 and then placed on the receptacles containing distilled water for evaluation of water vapour transmission. As mentioned earlier, the samples were weighed before and after each experiment wherein no significant change in the mass was observed. Therefore, it can be inferred that the water vapour was transmitted across directly without being engaged by the fabric, which can be attributed to the use of synthetic fibres, such as polyester, in the structure. Especially, the spacer yarn PVDF is highly hydrophobic and as such will not allow for any moisture uptake. As compared to the natural fibres, polyamide can readily uptake water, however, the silver coating

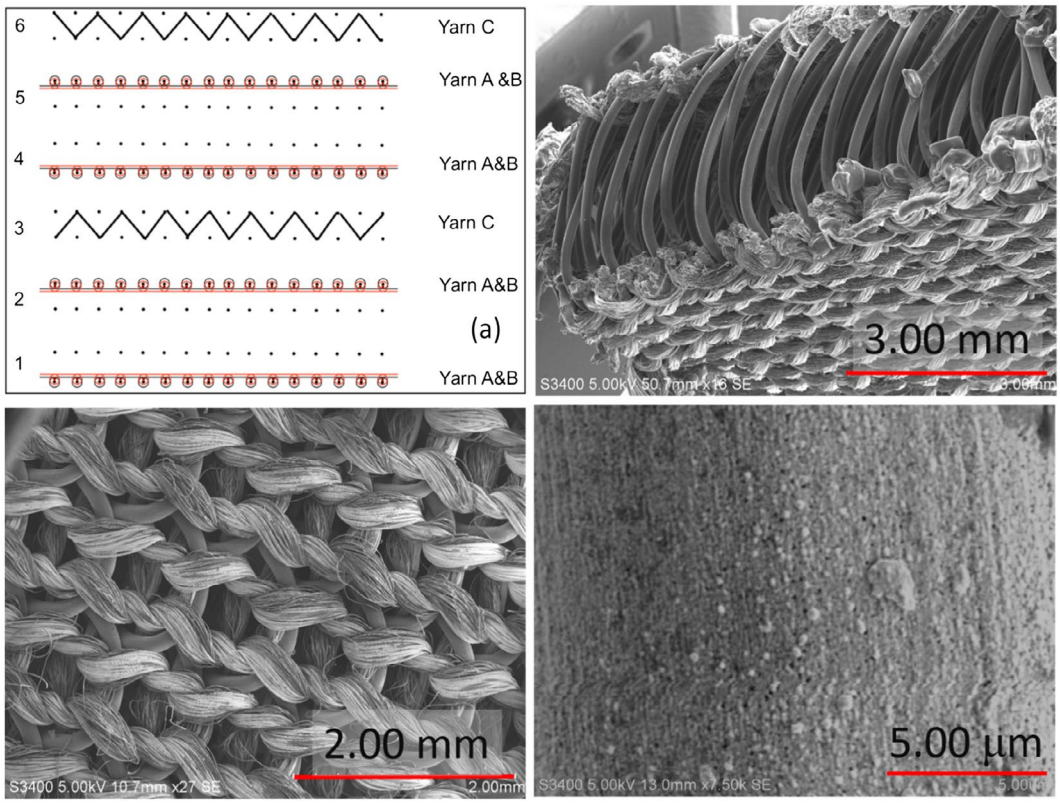

Figure 1. (a) Schematic of fabric structure with the position of various yarns in the structure, yarn C is the PVDF spacer whereas yarns A and B correspond to the Ag/PA66 and polyester plaiting yarns, (b) cross-sectional SEM image of the actual fabric clearly showing the position of piezoelectric and conductive yarns, (c) technical face of the fabric and (d) electroplated Ag on the Ag/PA66 yarns. Reproduced from Soin et al. (2014) with permission from The Royal Society of Chemistry.

on the PA66 fibres can potentially hinder the water uptake. As the 3-D fabric samples were kept in standard laboratory conditions (20 °C ± 2 and 65% ± 2% humidity) for 48 h before the tests, it can also be argued that the water uptake of the polyamide had already reached the equilibrium before the test itself. The mass of the test assembly was measured at the beginning of the test as well as after 24-h periods. Graph given in Figure 2, presents the decrease in total mass related to elapsed time *i.e.* the decrease in the mass of the test assembly provides information on how much water vapour is transmitted through the fabric in 24, 48, 72 and 96 h. The amount of the water vapour transmitted through the fabric increases with the increase in time with the calculated transmitted water vapour value (Equation 2) of 1.34 g/m^2/day.

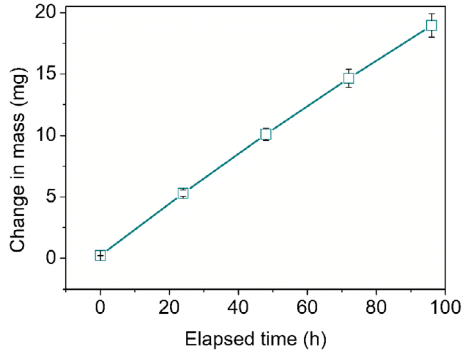

Figure 2. Total mass change (mg) of the test assembly, prepared for water vapour permeability test, measured after 0, 24, 48, 72 and 96 h.

The bursting strength measurement of the 3-D fabric samples was carried out according to TS 393 EN ISO 13,938–1 standard. Measurements in triplicate showed that a pressure higher than 2400 kPa is needed before the fabric bursts. This value is remarkably high as compared to 2-D knitted fabric structures. Bursting strength of 11 2-D knitted sportech fabrics were reported in the literature and they were found to be between ~ 390 kPa and ~ 580 kPa in the literature (Gürkan Ünal & Üreyen, 2016). The wear abrasion performance of the piezoelectric fabrics was investigated by rubbing the fabric samples onto the abradant fabric at an applied weight of 12 kPa. Even though the plaiting of the yarns was done in exactly the same manner for both the faces, there was a slight visual difference in the two technical faces of the fabric as seen in Figure 3. A 'yellow' tone was dominant at one side, while a 'grey' tone was dominant at the other side and therefore, the wear abrasion tests was carried out for both the sides. Visuals of the samples after each 10,000 rubs are given in Figure 4(a-l). Small pilings were detected after 18,000 rubs, with an increase observed in their size and number with an increase in the rubbing cycles. However, no broken yarns or holes were observed for up to 60,000 rubs as seen in the Figure 4(a-l). The wear abrasion of a textile structure can also be explained by the change in weight after wear abrasion test (Figure 4(m)). After 60,000 rubs, the sample whose grey toned side was subjected to friction lost about 3 mg of its weight, while the yellow toned side sample lost 2 mg of its weight. However, there was not any visible yarn breakage or hole in the fabric. Since the used materials in presented 3-D piezoelectric spacer fabric were synthetic textile yarns and filaments, pile loss is not expected and could

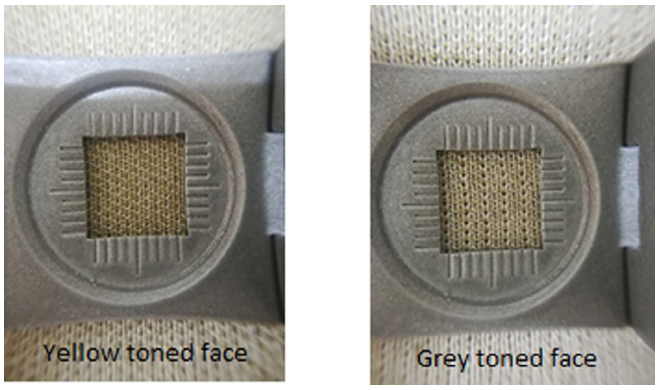

Figure 3. Visual of the colour difference between two faces of the spacer fabric, investigated under a loop. More of the polyester yarn is visible on the surface of the 'grey' toned side as compared to the 'yellow' toned side.

be attributed to the potential loss of Ag from Ag/PA66 yarns. To this effect, we have measured the surface resistance of the pristine technical faces of the fabric as well as at regular intervals during the rubbing cycles. As seen from Figure 4(n), there is a systematic increase in the surface resistance of the abraded fabric samples which can only occur due to the loss of Ag from the Ag/PA66 yarns. With the increased number of friction cycles, fibrillation/fraying of the Ag/PA66 fibres was observed (see Figure 5(d,h)) which can potentially cause the removal of loose fibres and consequentially an increase in the surface resistance.

The antibacterial activity of 3-D piezoelectric fabrics was examined against *E.coli* and *S.aureus* (Figure 6). *E.coli* and *S.aureus* cells were exposed to 3-D piezoelectric fabric in PBS solution for 3 h. Cell viability was determined by spot assay (Figure 6(a,b)) dilution and spread plate method (Figure 6(c)) discussed earlier in the experimental section. Three-dimensional piezoelectric fabrics were found to be more potent against *E.coli* as we could not find any colony in any of the dilution factor Figure 6(a), also no growth was observed on the spread plate Figure 6(c). In contrast, control experiments performed in the absence of 3-D piezoelectric fabrics showed growth in all the dilutions (Figure 6(a)). However, in case of *S. aureus,* the antibacterial efficacy of 3-D piezoelectric fabric was found to be reduced in comparison to *E. coli*. As shown in Figure 6(b), colonies were present at lower dilution whereas on increasing the dilution no colony formation was observed in *S. aureus* cells treated with 3-D piezoelectric fabrics. In case of untreated (control) *S. aureus* cells growth was observed in all the dilutions in spot assay. We can also conclude that at higher cell number (i.e. at lower dilution) colonies were present, however, at lower cell number (i.e. at higher dilution) no growth was observed as corroborated by our spot assay result in Figure 6(b). Thus, confirming the antibacterial activity of 3-D piezoelectric fabrics.

The results revealed that silver coated 3-D piezoelectric fabrics exhibit antibacterial activity against not only Gram-negative bacteria *E. coli* but it is also capable of killing antibiotic methicillin-resistant bacteria *S. aureus* (Stapleton & Taylor, 2002). The

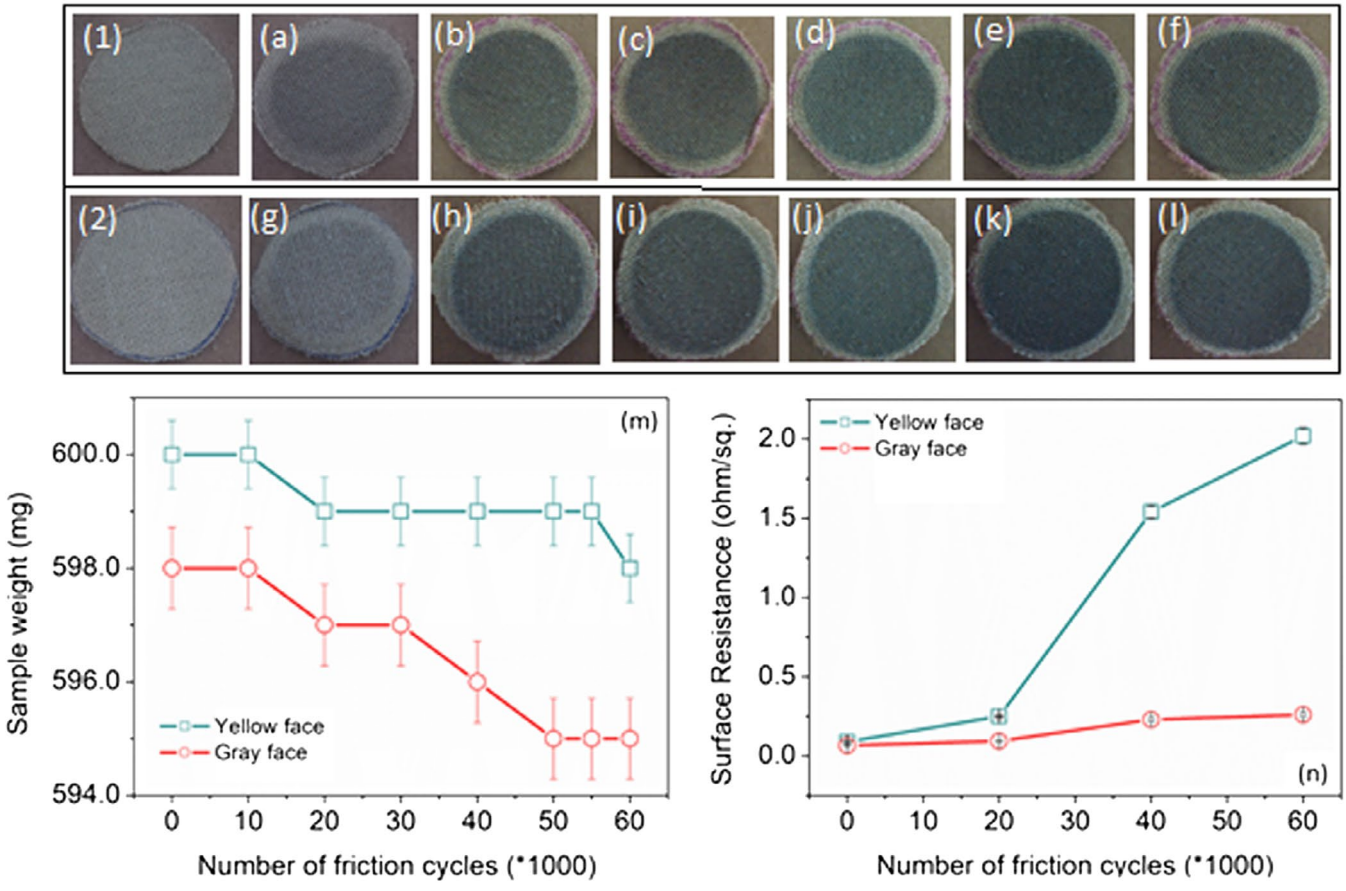

Figure 4. Digital photographs of the 3-D piezoelectric fabrics taken before the wear test (1,2) and after each 10,000 rubs for the (a-f) yellow face and (g-l) grey face, under an applied weight of 12 kPa. The corresponding change in the (m) weight and (n) sheet resistance of the two fabric faces as a function of number of friction cycles.

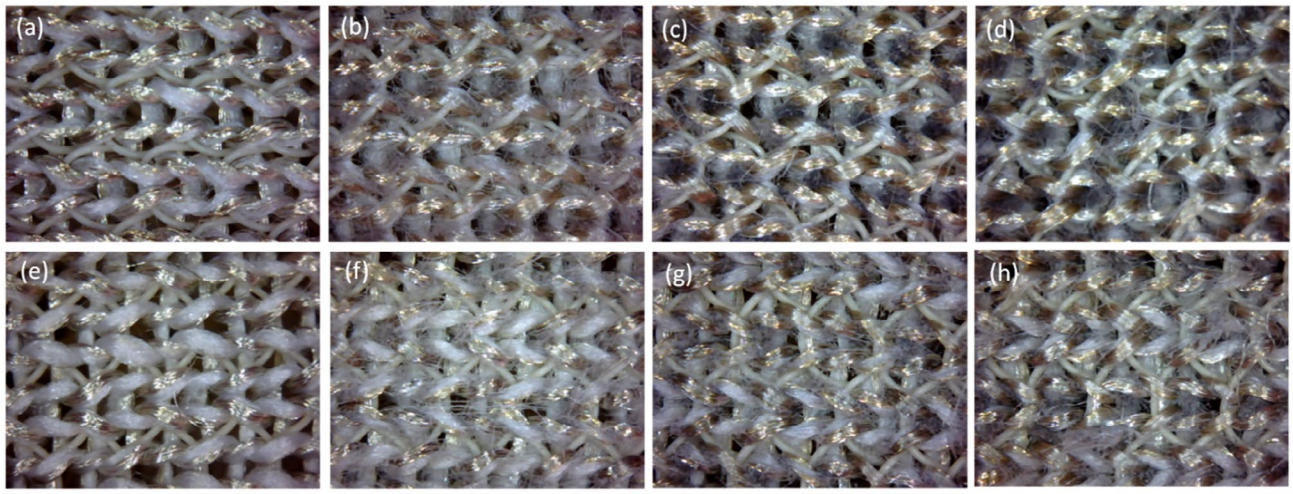

Figure 5. Digital photographs of the (a-d) yellow face and (e-h) grey face of the 3-D piezoelectric fabrics. (a) and (e) were taken before the test (unrubbed samples), while (b-d) and (f-h) were taken after each 20,000 rubs showing the fraying of the Ag/PA66 fibres after rubbing tests.

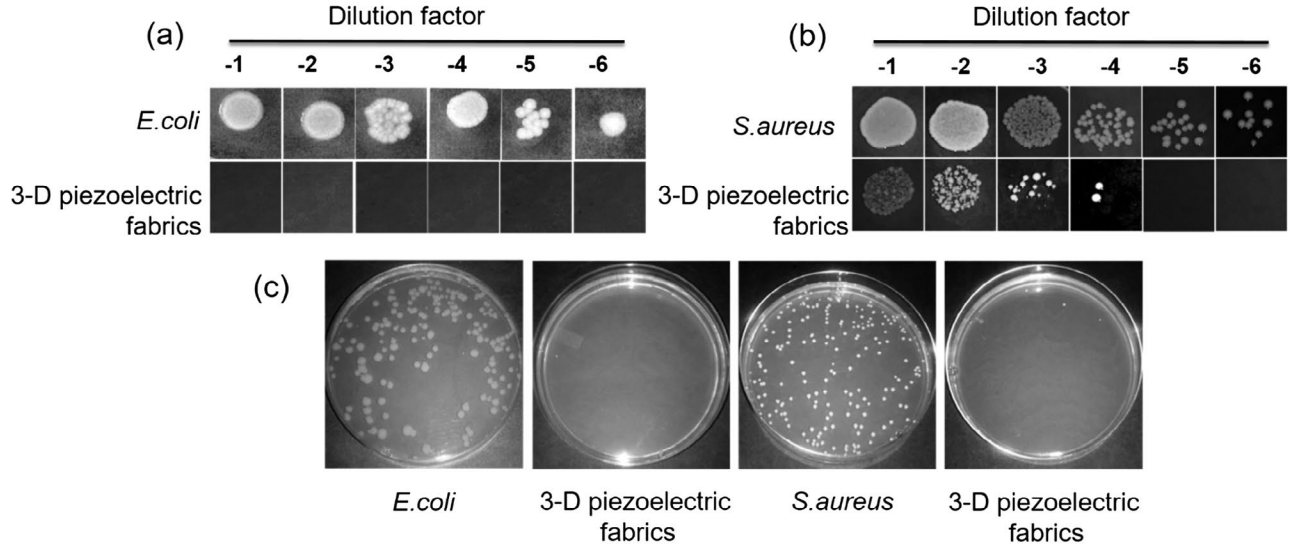

Figure 6. Antibacterial activity of 3-D piezoelectric fabrics (a, b) Spot assay analysis showing antibacterial activity of 3-D piezoelectric fabrics against *E. coli* and *S. aureus*. After treatment with 3-D piezoelectric fabrics 100 µl of the culture was 10-fold serially diluted and 5 µl of each of the dilutions was spotted on LB agar plates. E.*coli* and *S. aureus* cells, which were not treated with 3-D piezoelectric fabrics, served as control for the experiment, (c) Digital micrographs representing antibacterial activity of 3-D piezoelectric fabrics against *E. coli* and *S. aureus*. 100 µl of *E. coli* and *S. aureus* cells treated with 3-D piezoelectric fabrics were spread directly on the LB agar plates. Untreated *E. coli* and *S ureus* cells plated on LB agar plates were taken as control.

3-D silver-coated fabric is found to be less potent as antibacterial against Gram-positive bacteria *S. aureus,* as compared to the Gram-negative bacteria *E. coli*; this observation is in well agreement with several previously published reports. Previously, several studies have reported better antibacterial activity of the silver nanoparticles against Gram-negative bacteria, as compared to the Gram-positive bacteria *S. Aureus* (Kim, Lee, Ryu, Choi, & Lee, 2011; Cavassin et al., 2015; Taglietti et al., 2012; Amato *et al.*, 2011). The reason behind better bacteriocidal activity of the Ag against *S. aureus* compare to the *E. coli* is believed to be because of the complex cell membrane structure of the *S. aureus* compare to *E. coli*. The *S. aureus* contains thick lipoteichoic acid containing peptidoglycan layer and cell membrane as compared to the *E. coli* (Kim et al., 2011). The thickness of the peptidoglycan layer for *S. aureus* and *E. coli* is estimated to be in the range of 20–80 nm and 7–8 nm, respectively. The thicker peptidoglycan layer of the *S. aureus* provides it better protection compared to the *E. coli* against the attack of the reactive oxygen species *(ROS)* generated by the silver. Thus, the 3-D fabric samples are highly effective in stopping the growth and propagation of both the Gram-positive and Gram-negative bacteria and as such could be used for fabrication of smart functional textiles with antibacterial properties.

Conclusions

The as-prepared 3-D knitted piezoelectric spacer fabric was tested for its fabric performances and antibacterial properties. The thickness, mass and porosity of the fabric were measured and found to be 3.51 mm, 485 g/m^2 and 68%, respectively. Both

the air permeability and water vapour transmission test results revealed that 3-D knitted piezoelectric spacer fabric is both air and water vapour permeable owing to its porous structure. The resistance to wear abrasion test results showed that the fabric could easily endure over 60,000 rubs, applied at 12 kPa with a high bursting strength of more than 2400 kPa. Furthermore, the antibacterial activity of 3-D piezoelectric fabrics was examined against *E.coli* and *S.aureus* with the results showing that the 3-D piezoelectric fabric was more efficient against *E.coli* in comparison to *S.aureus*. The tests conducted during the course of the work reveal that the newly introduced multifunctional 3-D knitted piezoelectric spacer fabric has good fabric performance features for providing long-term durability for enabling technical applications such as wearable energy harvesters with inherent antibacterial properties.

Acknowledgements

The authors would like to thank Dr Erhan Sancak and Dr Mustafa Sabri Ozen at the Department of Textile Engineering, Faculty of Technology, Marmara University, Istanbul, Turkey for their help in electrical measurements.

Disclosure statement

No potential conflict of interest was reported by the authors.

References

Amato, E., Diaz-Fernandez, Y. A., Taglietti, A., Pallavicini, P., Pasotti, L., Cucca, L., … Necchi, V. (2011). Synthesis, characterization and antibacterial activity against gram positive and gram negative bacteria of biomimetically coated silver nanoparticles. *Langmuir: the ACS journal of surfaces and colloids*, *27*(15), 9165–9173.

Anand, S. C., & Rajendran, S. (2011). *Development of 3D structures for venous leg ulcer management*. Third World Conference on 3D Fabrics and Their Applications, Wuhan.

Arabuli, S., Vlasenko, V., Havelka, A., & Kus, Z. (2010). Analysis of modern methods for measuring vapor permeability properties of textiles. 7, Liberec.

Arumugam, V., Mishra, R., Militky, J., Davies, L., & Slater, S. (2017). Thermal and water vapor transmission through porous warp knitted 3D spacer fabrics for car upholstery applications. *The Journal of The Textile Institute, 108*(7), 1095–1105.

Bayramol, D. V., Soin, N., Shah, T., Siores, E., Matsouka, D., & Vassiliadis, S. (2017). Energy harvesting smart textiles. *Smart Textiles Fundamentals, Design, and Interaction,* 199–231 içinde Springer.

Cavassin, E. D., de Figueiredo, L. F., Otoch, J. P., Seckler, M. M., de Oliveira, R. A., Franco, F. F., & Costa, S. F. (2015). Comparison of methods to detect the *in vitro* activity of silver nanoparticles (AgNP) against multidrug resistant bacteria. *Journal of Nanobiotechnology, 13*(64), 1–16.

Chen, F., Liu, Y., & Hu, H. (2016). An experimental study on vibration isolation performance of weft-knitted spacer fabrics. *Textile Research Journal, 86*(20), 2225–2235.

Crina, B., Blaga, M., Luminita, V., & Mishra, R. (2013). Comfort properties of functional weft knitted spacer fabrics. *Tekstil ve Konfeksiyon, 23*(2), 220–227.

Delkumburewatte, G. B., & Dias, T. (2009). Porosity and capillarity of weft knitted spacer structures. *Fibers and Polymers, 10*(2), 226–230.

Dias, T., Monaragala, R., Needham, P., & Lay, E. (2007). Analysis of sound absorption of tuck spacer fabrics to reduce automotive noise. *Measurement Science and Technology, 18*(8), 2657–2666.

Fang, J., Niu, H., Wang, H., Wang, X., & Lin, T. (2013). Enhanced mechanical energy harvesting using needleless electrospun poly(vinylidene fluoride) nanofibre webs. *Energy & Environmental Science, 6*(7), 2196–2202.

Fangueiro, R. E., & Soutinho, H. F. (2013, February 28). *U. S. Patent No. US 201,300,524,26, A1*.

Gong, R. H., Dong, Z., & Porat, I. (2003). Novel technology for 3D nonwovens. *Textile Research Journal, 73*, 120–123.

Großmann, K., Mühl, A., Löser, M., Cherif, C., Hoffmann, G., & Torun, A. R. (2010). New solutions for the manufacturing of spacer preforms for thermoplastic textile-reinforced lightweight structures. *Production Engineering, 4*(6), 589–597.

Gürkan Ünal, P., & Üreyen, M. E. (2016). Mechanical and permeability properties of sportech fabrics. *Industria Textila, 67*(3), 151–156.

Kim, S.-H., Lee, H.-S., Ryu, D.-S., Choi, S.-J., & Lee, D.-S. (2011). Antibacterial activity of silver-nanoparticles against Staphylococcus aureus and Escherichia coli. *Korean Journal of Microbiology and Biotechnology, 39*(1), 77–85.

Li, M., Wang, S., Zhang, Z., & Wu, B. (2009). Effect of structure on the mechanical behaviors of three-dimensional spacer fabric composites. *Applied Composite Materials, 16*(1), 1–14.

Liu, Y., & Hu, H. (2011). Compression property and air permeability of weft-knitted spacer fabrics. *The Journal of The Textile Institute, 102*(4), 366–372.

Liu, Y., Hu, H., Long, H., & Zhao, L. (2012). Impact compressive behavior of warp-knitted spacer fabrics for protective applications. *Textile Research Journal, 82*(8), 773–788.

Mountasir, A., Hoffmann, G., & Cherif, C. (2011). Development of weaving technology for manufacturing three-dimensional spacer fabrics with high-performance yarns for thermoplastic composite applications: An analysis of two-dimensional mechanical properties. *Textile Research Journal, 81*(13), 1354–1366.

Pereira, S., Anand, S. C., Rajendran, S., & Wood, C. (2007). A study of the structure and properties of novel fabrics for knee braces. *Journal of Industrial Textiles, 36*(4), 279–300.

Rajan, T. P., Souza, L. D., Ramakrishnan, G., & Zakriya, G. M. (2016). Comfort properties of functional warp-knitted polyester spacer fabrics for shoe insole applications. *Journal of Industrial Textiles, 45*(6), 1239–1251.

Shepherd, A. A. (2004, August 24). *USA Patent No. US 6779369, B2*.

Soin, N., Anand, S. C., & Shah, T. H. (2016). Energy harvesting and storage textiles. *Handbook of technical textiles: technical textile applications,* 357–396 içinde Woodhead Publishing.

Soin, N., Shah, T. H., Anand, S. C., Geng, J., Pornwannachai, W., Mandal, P., & Siores, E. (2014). Novel "3-D spacer" all fibre piezoelectric textiles for energy harvesting applications. *Energy & Environmental Science, 7*(5), 1670–1679.

Stapleton, P. D., & Taylor, P. W. (2002). Methicillin resistance in Staphylococcus aureus: mechanisms and modulation. *Science Progress, 85*(1), 57–72.

Stempien, Z., Rybicki, T., & Rybicki, E. (2015). In-situ deposition of polyaniline and polypyrrole electroconductive layers on textile surfaces by the reactive ink-jet printing technique. *Synthetic Metals, 202*, 49–62.

Taglietti, A., Fernandez, Y. A., Amato, E., Cucca, L., Dacarro, G., Grisoli, P., . . . Patrini, M. (2012). Antibacterial activity of glutathione-coated silver nanoparticles against gram positive and gram negative bacteria. *Langmuir: the ACS journal of surfaces and colloids, 28*(21), 8140–8148.

Ünal, P. G. (2012). 3D Woven Fabrics. *Woven Fabrics,* 91–120 içinde Intech Open Access Publication.

Wollina, U., Heide, M., Müller-Litz, W., Obenauf, D., & Ash, J. (2003). Functional textiles in prevention of chronic wounds, wound healing and tissue engineering. *Textiles and the Skin, 31*, 82–97.

Wollina, U., Heide, M., & Swere, M. (2002). Spacer fabrics – a potential tool in the prevention of chronic wounds. *Exogenous Dermatology, 1*(6), 276–278.

Yang, Y., & Hu, H. (2016). Spacer fabric-based exuding wound dressing – Part I: Structural design, fabrication and property evaluation of spacer fabrics. *Textile Research Journal, 87*, 1–12.

Ye, X., Fangueiro, R., Hu, H., & de Araújo, M. (2007). Application of warp-knitted spacer fabrics in car seats. *The Journal of The Textile Institute, 98*(4), 337–344.

Ye, X., Ho, H., & Feng, X. (2008). Development of the warp knitted spacer fabrics for cushion applications. *Journal of Industrial Textiles, 34*(3), 213–223.

Zeng, W., Tao, X.-M., Chen, S., Shang, S., Chan, H. L., & Choy, S. H. (2013). Highly durable all-fiber nanogenerator for mechanical energy harvesting. *Energy and Environmental Science, 6*(9), 2631–2638.